pseudogenes as a consequence of an evolutionary bottleneck that may have accompanied the colonization process.

The genome sequence of *Y. pestis* reveals a pathogen that has undergone considerable genetic flux, with evidence of selective genome expansion by lateral gene transfer of plasmid and chromosomal genes, and subsequent initial stages of genome size reduction. We believe that these features correlate with a change in pathogenic niche, and therefore this genome sequence provides a unique insight into the genetic events that are associated with the emergence of a new pathogenic species. The newly emerged pathogen is highly virulent for humans, causing pandemics of systemic, and often fatal, disease, contrasting with the ancestral species that evolved to cause non-fatal enteritis in similar hosts. □

Methods

A single colony of *Y. pestis* strain CO92 was picked from Congo Red agar and grown overnight in BAB broth with shaking at 37 °C. Cells were collected and total DNA (10 mg) was isolated using proteinase K treatment followed by phenol extraction. The DNA was fragmented by sonication, and several libraries were generated in pUC18 using size fractions ranging from 1.0 to 2.5 kb. The whole genome sequence was obtained from 94,881 end sequences (giving 9.6× coverage) derived from these libraries using dye terminator chemistry on ABI377 automated sequencers. End sequences from larger insert plasmid (pSP64; 3.1× clone coverage, 9–11 kb insert size) and lambda (lambda-FIX-II; 4.0× clone coverage, 20–22 kb insert size) libraries were used as a scaffold. The sequence was assembled, finished and annotated as described previously[30], using the program Artemis (http://www.sanger.ac.uk/Software/Artemis) to collate data and facilitate annotation. The genome sequences of *Y. pestis* and *E. coli* were compared pairwise using the Artemis Comparison Tool (ACT) (http://www.sanger.ac.uk/Software/ACT). Pseudogenes had one or more mutations that would ablate expression; each of the inactivating mutations was subsequently checked against the original sequencing data.

Received 8 May; accepted 16 August 2001.

1. Perry, R. D. & Fetherston, J. D. *Yersinia pestis*—etiologic agent of plague. *Clin. Microbiol. Rev.* **10,** 35–66 (1997).
2. Galimand, M. *et al.* Multidrug resistance in *Yersinia pestis* mediated by a transferable plasmid. *N. Engl. J. Med.* **337,** 677–680 (1997).
3. Skurnik, M., Peippo, A. & Ervela, E. Characterization of the O-antigen gene clusters of *Yersinia pseudotuberculosis* and the cryptic O-antigen gene cluster of *Yersinia pestis* shows that the plague bacillus is most closely related to and has evolved from *Y. pseudotuberculosis* serotype O:1b. *Mol. Microbiol.* **37,** 316–330 (2000).
4. Achtman, M. *et al. Yersinia pestis*, the cause of plague, is a recently emerged clone of *Yersinia pseudotuberculosis*. *Proc. Natl Acad. Sci. USA* **96,** 14043–14048 (1999).
5. Doll, J. M. *et al.* Cat-transmitted fatal pneumonic plague in a person who traveled from Colorado to Arizona. *Am. J. Trop. Med. Hyg.* **51,** 109–114 (1994).
6. Lobry, J. R. Asymmetric substitution patterns in the two DNA strands of bacteria. *Mol. Biol. Evol.* **13,** 660–665 (1996).
7. Guiyoule, A. *et al.* Recent emergence of new variants of *Yersinia pestis* in Madagascar. *J. Clin. Microbiol.* **35,** 2826–2833 (1997).
8. Cowan, C., Jones, H. A., Kaya, Y. H., Perry, R. D. & Straley, S. C. Invasion of epithelial cells by *Yersinia pestis*: evidence for a *Y. pestis*-specific invasin. *Infect. Immun.* **68,** 4523–4530 (2000).
9. Prentice, M. B. *et al. Yersinia pestis* pFra shows biovar-specific differences and recent common ancestry with a *Salmonella enterica* serovar Typhi plasmid. *J. Bacteriol.* **183,** 2586–2594 (2001).
10. Hinnebusch, J. *et al.* Murine toxin of *Yersinia pestis* shows phospholipase D activity but is not required for virulence in mice. *Int. J. Med. Microbiol.* **290,** 483–487 (2000).
11. Buchrieser, C. *et al.* The 102-kilobase *pgm* locus of *Yersinia pestis*: sequence analysis and comparison of selected regions among different *Yersinia pestis* and *Yersinia pseudotuberculosis* strains. *Infect Immun.* **67,** 4851–4861 (1999).
12. Waterfield, N. R., Bowen, D. J., Fetherston, J. D., Perry, R. D. & ffrench-Constant, R. H. The *tc* genes of *Photorhabdus*: a growing family. *Trends Microbiol.* **9,** 185–191 (2001).
13. Wang, P. & Granados, R. R. An intestinal mucin is the target substrate for a baculovirus enhancin. *Proc. Natl Acad. Sci. USA* **94,** 6977–6982 (1997).
14. Cornelis, G. R. *et al.* The virulence plasmid of *Yersinia*, an antihost genome. *Microbiol. Mol. Biol. Rev.* **62,** 1315–1352 (1998).
15. Shea, J. E., Hensel, M., Gleeson, C. & Holden, D. W. Identification of a virulence locus encoding a second type III secretion system in *Salmonella typhimurium*. *Proc. Natl Acad. Sci. USA* **93,** 2593–2597 (1996).
16. Haller, J. C., Carlson, S., Pederson, K. J. & Pierson, D. E. A chromosomally encoded type III secretion pathway in *Yersinia enterocolitica* is important in virulence. *Mol. Microbiol.* **36,** 1436–1446 (2000).
17. Townsend, S. M. *et al. Salmonella enterica* serovar Typhi possesses a unique repertoire of fimbrial gene sequences. *Infect. Immun.* **69,** 2894–2901 (2001).
18. Odaert, M., Berche, P. & Simonet, M. Molecular typing of *Yersinia pseudotuberculosis* by using an IS*200*-like element. *J. Clin. Microbiol.* **34,** 2231–2235 (1996).
19. McDonough, K. A. & Hare, J. M. Homology with a repeated *Yersinia pestis* DNA sequence IS100 correlates with pesticin sensitivity in *Yersinia pseudotuberculosis*. *J. Bacteriol.* **179,** 2081–2085 (1997).
20. Lerm, M., Schmidt, G. & Aktories, K. Bacterial protein toxins targeting rho GTPases. *FEMS Microbiol. Lett.* **188,** 1–6 (2000).
21. Henderson, I. R., Owen, P. & Nataro, J. P. Molecular switches—the ON and OFF of bacterial phase variation. *Mol. Microbiol.* **33,** 919–932 (1999).
22. Sebbane, F., Devalckenaere, A., Foulon, J., Carniel, E. & Simonet, M. Silencing and reactivation of urease in *Yersinia pestis* is determined by one G residue at a specific position in the *ureD* gene. *Infect. Immun.* **69,** 170–176 (2001).
23. Young, G. M., Badger, J. L. & Miller, V. L. Motility is required to initiate host cell invasion by *Yersinia enterocolitica*. *Infect. Immun.* **68,** 4323–4326 (2000).
24. Darwin, A. J. & Miller, V. L. Identification of *Yersinia enterocolitica* genes affecting survival in an animal host using signature-tagged transposon mutagenesis. *Mol. Microbiol.* **32,** 51–62 (1999).
25. Nesper, J. *et al.* Characterization of *Vibrio cholerae* O1 El tor *galU* and *galE* mutants: influence on lipopolysaccharide structure, colonization, and biofilm formation. *Infect. Immun.* **69,** 435–445 (2001).
26. Wachtel, M. R. & Miller, V. L. *In vitro* and *in vivo* characterization of an *ail* mutant of *Yersinia enterocolitica*. *Infect. Immun.* **63,** 2541–2548 (1995).
27. Torosian, S. & Zsigray, R. in *Abstracts of the 96th General Meeting of the American Society of Microbiology 1996* Abstract B-13, 191 (American Society for Microbiology, Washington DC, 1996).
28. Pierson, D. E. Mutations affecting lipopolysaccharide enhance *ail*-mediated entry of *Yersinia enterocolitica* into mammalian cells. *J. Bacteriol.* **176,** 4043–4051 (1994).
29. Mecsas, J., Bilis, I. & Falkow, S. Identification of attenuated *Yersinia pseudotuberculosis* strains and characterization of an orogastric infection in BALB/c mice on day 5 postinfection by signature-tagged mutagenesis. *Infect. Immun.* **69,** 2779–2787 (2001).
30. Parkhill, J. *et al.* Complete DNA sequence of a serogroup A strain of *Neisseria meningitidis* Z2491. *Nature* **404,** 502–506 (2000).

Supplementary information is available on *Nature*'s World-Wide Web site (http://www.nature.com) or as paper copy from the London editorial office of *Nature*.

Acknowledgements

We acknowledge the support of the Sanger Centre core sequencing, subcloning and informatics groups. This work was funded by the Wellcome Trust through its Beowulf Genomics initiative. We are grateful to E. Garcia of the *Y. pseudotuberculosis* sequencing group at the Lawrence Livermore National Laboratories for giving permission to use sequence data before they are published. B.W.W. and A.V.K. are supported by the Wellcome Trust.

Correspondence and requests for materials should be addressed to J.P. (e-mail: parkhill@sanger.ac.uk) or B.W.W. (e-mail: brendan.wren@lshtm.ac.uk). The sequences have been submitted to EMBL under the accession numbers AL590842 (chromosome), AL109969 (pPCP1), AL117189 (pCD1) and AL117211 (pMT1).

An endogenous cannabinoid (2-AG) is neuroprotective after brain injury

David Panikashvili*†, Constantina Simeonidou*, Shimon Ben-Shabat†, Lumír Hanuš†, Aviva Breuer†, Raphael Mechoulam† & Esther Shohami*

** Department of Pharmacology, and † Department of Medicinal Chemistry and Natural Products, Medical Faculty, Hebrew University, Jerusalem 91120, Israel*

Traumatic brain injury triggers the accumulation of harmful mediators that may lead to secondary damage[1,2]. Protective mechanisms to attenuate damage are also set in motion[2]. 2-Arachidonoyl glycerol (2-AG) is an endogenous cannabinoid, identified both in the periphery[3] and in the brain[4], but its physiological roles have been only partially clarified[5–7]. Here we show that, after injury to the mouse brain, 2-AG may have a neuroprotective role in which the cannabinoid system is involved. After closed head injury (CHI) in mice, the level of endogenous 2-AG was significantly elevated. We administered synthetic 2-AG to mice after CHI and found significant reduction of brain oedema, better clinical recovery, reduced infarct volume and reduced hippocampal cell death compared with controls. When 2-AG was administered together with additional inactive 2-acyl-glycerols that are normally present in the brain, functional recovery was significantly enhanced. The beneficial effect of 2-AG was dose-dependently attenuated by SR-141761A, an antagonist of the CB_1 cannabinoid receptor.

Traumatic brain injury is a major cause of mortality and morbidity, yet there is no effective drug to treat brain-injured patients. Understanding post-trauma events and developing neuroprotective agents are therefore important[8]. Cannabinoids act through two distinct receptors, one of which (CB_1) is found mainly in the brain. We have previously reported that 2-AG suppresses formation of reactive oxygen species (ROS) and tumour necrosis factor-α (TNF-α) by murine macrophages

in vitro after stimulation with lipopolysaccharide (LPS), and have noted lower levels of TNF-α in the serum of LPS-treated mice after administration of 2-AG[9]. Both classes of mediators, ROS[10] and TNF-α[11], are major contributors to the pathophysiology of brain injury.

On the basis of these observations, we assumed that 2-AG could have a neuroprotective role in the post-traumatic brain. We therefore investigated the dynamic changes in brain 2-AG levels after traumatic brain injury; the possibility that exogenous 2-AG may attenuate brain damage after CHI; and the involvement of the CB_1 receptor in neuroprotection.

Mice were subjected to CHI using a weight-drop device, or to sham surgery, as described elsewhere[12]. They were decapitated at various time intervals (15 min, 1, 4, 8 or 24 h) and the brains were removed within 1 min and frozen in liquid nitrogen. The rapid freezing minimized the post-mortem production of 2-AG. This was confirmed by the similar levels of 2-AG obtained in brains extracted at 1, 3 or 5 min after decapitation (data not shown). The levels of brain 2-AG were determined in the traumatized hemispheres (Fig. 1) and compared with those in controls. One hour after CHI the levels of 2-AG were already significantly higher than in sham, non-injured mice, peaking at a tenfold increase after 4 h, and declining thereafter. Even after 24 h, the levels of 2-AG were still higher (sixfold) than in controls. In the contralateral hemisphere, the changes in 2-AG were minor, and not significant (data not shown).

To test the role of 2-AG in post-traumatic pathophysiology, we synthesized 2-AG as previously described[3] and intravenously administered doses of 0.1, 5 and 10 mg kg^{-1} 15 min after CHI. One of the early manifestations of brain injury is oedema formation (accumulation of water in the tissue), leading to increased intracranial pressure. We therefore examined the effect of 2-AG on oedema formation by measuring water content 24 h after trauma, the time of maximal oedema[12]. At all doses tested, 2-AG significantly reduced water accumulation by about 50% (Fig. 2a).

The clinical status of the mice was evaluated 1 and 24 h after CHI using a scoring system testing motor and behavioural functions[13] (neurological severity score, NSS: 0, healthy, to 10, fatally injured). The initial NSS (at 1 h) reflects the severity of injury, and ΔNSS, the difference between the score at 1 and 24 h, reflects recovery. Whereas the NSS (1 h) was similar in the treated and control groups (8.25 ± 0.36 and 7.63 ± 0.46, respectively), the mice treated with 2-AG recovered faster within the first 24 h. All doses of 2-AG showed a trend towards better recovery (greater ΔNSS), but it reached significance only at 5 mg kg^{-1} ($P < 0.01$, versus control; Fig. 2b). The effect of 2-AG was not long lasting. We injected 2-AG 1 h after CHI, and evaluated NSS 1, 4 and 7 days later, but found significant protection on the first day only, and not on subsequent days (Fig. 2c). Brain oedema and neurological deficits are not necessarily interdependent, because they represent different manifestations of brain damage. Indeed, we found that 2-AG is less potent against the motor deficits than in reducing oedema, as evidenced from the different effective doses needed to achieve protection.

One of the manifestations of brain injury is neuronal cell death, which is grossly evidenced by an infarct around the site of injury. Mice were treated with either 2-AG (5 mg kg^{-1}, $n = 7$) or vehicle ($n = 12$), decapitated 24 h later and their brains were examined for changes in infarct volume[14]. Infarct volume was significantly reduced in 2-AG-treated mice compared with that in vehicle-treated mice (5.6 ± 1.2% and 10.2 ± 1.1%, respectively, of total brain volume; $P = 0.021$). No infarct was observed in sham-operated mice (data not shown). In addition, we examined the effect of 2-AG on hippocampal cell death, which occurs specifically in the CA3 subfield[12]. Mice were treated with vehicle or with 5 mg kg^{-1} of 2-AG

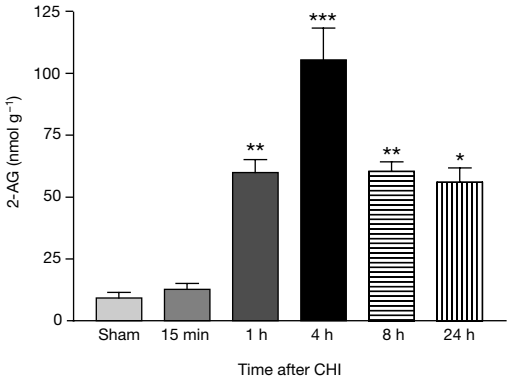

Figure 1 Temporal profile of 2-AG changes after CHI. CHI was induced over the left cerebral hemisphere. At the designated times the mice were killed and 2-AG was extracted from the contused hemisphere, separated on TLC and analysed by GC–MS. 2-AG levels were already significantly elevated 1 h after CHI, peaking at 4 h and sustained until 24 h. Controls are sham, non-injured mice. An analysis of variance (ANOVA) ($F = 36.01$, $P < 0.001$) with Tukey's *post hoc* test were performed: single asterisk, $P < 0.05$ versus control; double asterisk, $P < 0.01$ versus control; triple asterisk, $P < 0.001$ versus control. Data are mean ± s.e.m.

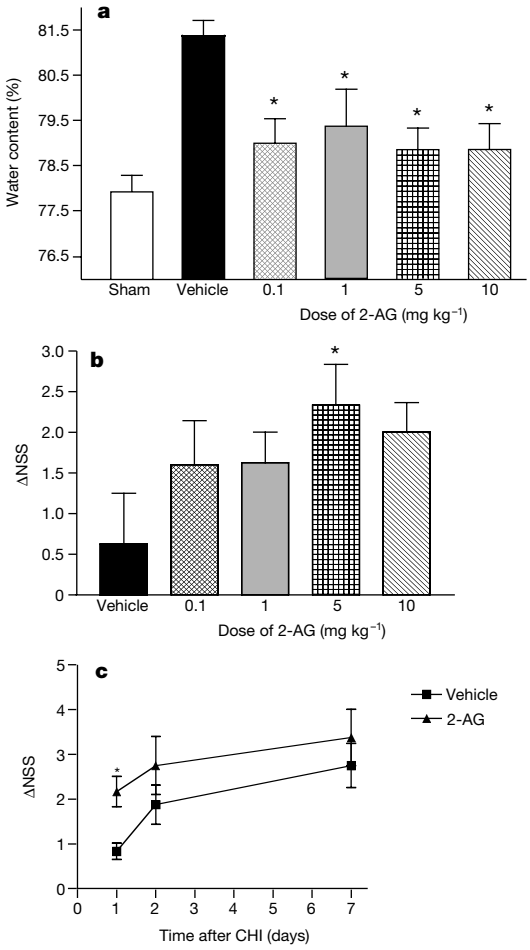

Figure 2 Protective effects of 2-AG after CHI. 2-AG was administered after CHI, and its protection against oedema formation (**a**) and effect on clinical recovery (**b**, **c**) are shown. **a**, 2-AG, at a dose range of 0.1–10 mg kg^{-1}, was injected 15 min after CHI, and tissue water content was evaluated 24 h later in the contused brain hemisphere. At all doses, 2-AG significantly reduced oedema. Controls are sham, non-injured mice and CHI-traumatized mice injected with vehicle. An ANOVA ($F = 5, 185$, $P < 0.001$) with Tukey's *post hoc* test were performed: asterisk, $P < 0.05$ versus control vehicle-injected CHI mice. **b**, ΔNSS reflects clinical recovery: a higher value indicates greater recovery. **c**, 2-AG (5 mg kg^{-1}) was injected 1 h after CHI and ΔNSS was assessed at 24 h, 48 h and 7 days. Data are mean ± s.e.m.

1 h after CHI, and killed 7 days later by perfusion fixation. Serial brain sections were stained with haematoxylin and eosin and Nissl. The ipsilateral hippocampus of vehicle- and 2-AG-treated mice showed ischaemic and dystrophic neurons, with large or small patchy acellular regions, in the CA3 subfield (Fig. 3). No neuronal pathology could be detected in the contralateral CA3 region (Fig. 3a, d). Neuronal loss was apparent in the injured side compared with the contralateral side of both vehicle- and 2-AG-treated mice (Fig. 4a); however, this loss was significantly more obvious in the vehicle-treated animals. The number of neurons counted in the CA3 area in the injured hemisphere, expressed as a percentage of those counted in the CA3 area in the intact hemisphere, was significantly lower in the vehicle-treated mice than in the 2-AG-treated mice (Fig. 4b).

2-AG is accompanied in mouse brains by an 'entourage' of congeners, such as 2-palmitoyl-glycerol and 2-linoleoyl-glycerol, which alone have no activity at the cannabinoid receptors. However, these glycerol esters facilitate the binding of 2-AG to the CB_1 and CB_2 receptors, probably through increasing the availability of 2-AG at the receptors by inhibiting its hydrolysis and uptake[15]. To test the effect of the entourage after CHI, mice were injected with a combination of 2-AG (1 mg kg^{-1}), 2-palmitoyl-glycerol (5 mg kg^{-1}) and 2-linoleoyl-glycerol (10 mg kg^{-1}) 1 h after CHI. Although no effect was observed when these compounds were injected separately, the combination of the three acyl-glycerol esters led to a significant improvement in functional recovery at 24 h (Fig. 5a). When the combination (2-AG plus entourage) was administered again 24 and 48 h after CHI, the improved clinical recovery was sustained up to 7 days after the trauma (Fig. 5b).

To determine whether the protective effect of the exogenous 2-AG is mediated at least in part by the CB_1 cannabinoid receptor, we injected SR-141716A, an antagonist specific to the CB_1 receptor subtype, after CHI, along with 2-AG. Oedema was determined 24 h later. Five groups of mice were subjected to CHI and treated with either vehicle (control), 2-AG (1 mg kg^{-1}) alone or with 3, 10 and 20 mg kg^{-1} of SR-141716A. The protective effect of 2-AG was dose-dependently attenuated by the antagonist (Fig. 6). The water content in mice treated with 2-AG and 20 mg kg^{-1} of antagonist did not differ from that in the CHI control mice. The doses of the antagonist used were relatively high; however, the effective dose could depend upon the species or strain of animal used in the study. High doses (≈20 mg kg^{-1}) of the antagonist have previously been used[16,17]. It should be noted, however, that the antagonist alone did not worsen the outcome of traumatized mice not treated with 2-AG (data not shown).

These results are, to our knowledge, the first to demonstrate temporal and local changes in brain levels of the endogenous cannabinoid 2-AG after traumatic brain injury and to record its neuroprotective effects. We have previously reported, using the same model of CHI, that the arachidonic acid metabolic cascade is activated after trauma[18], and that there is massive accumulation of calcium at the site of injury[19]. Both events may be related to 2-AG release. It seems that 2-AG can be synthesized and released from neuronal and non-neuronal cells on demand by a non-synaptic release mechanism[5]. Endocannabinoids are taken up by cells using a specific transporter[20] or, in particular for 2-AG, also by passive diffusion[5] and are hydrolysed by fatty acid amide hydrolase (FAAH), which acts on both anandamide and 2-AG[5,21].

Several cannabinoids that bind to CB_1 have been assayed for neuroprotection (mostly using *in vitro* models). 2-AG has been shown to protect cerebral neurons of rats from ischaemia *in vitro*[22], and cannabinoid receptor agonists inhibit glutamatergic synaptic transmission in hippocampal cultures *in vitro*[23]. The synthetic cannabinoid WIN 55212-2 decreases hippocampal neuronal loss after transient global cerebral ischaemia induced by occlusion of the middle cerebral artery in rats[24]. Indeed, our present findings show significant protection of hippocampal cells after treatment with 2-AG. Tetrahydrocannabinol was also shown to protect against

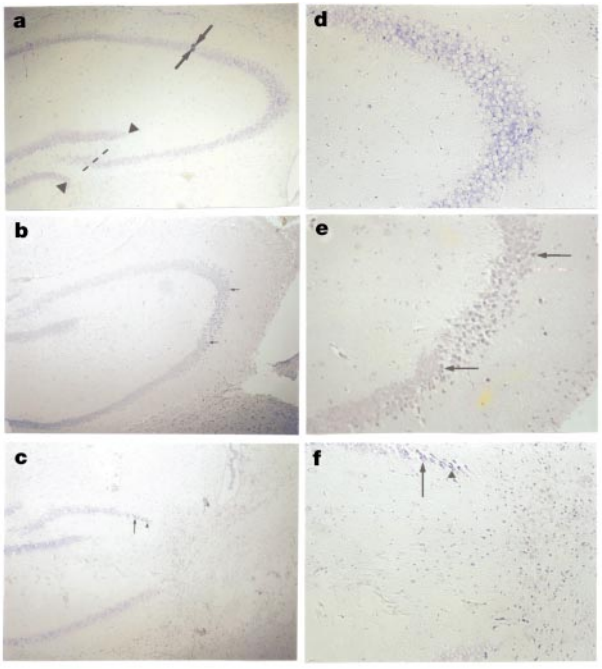

Figure 3 Hippocampal cell death after the effect of CHI is reduced by 2-AG. **a–c**, Low magnification; **d–f**, high magnification. **a**, **d**, The contralateral, uninjured side. The hippocampal CA3 subfield is outlined in **a**, from the CA3/2 border (arrows) up to the point at which the CA3 neurons enter the dentate gyrus (arrowheads). **b**, **e**, 2-AG-treated mice. Ischaemic neurons (arrows) are shown in the injured hippocampus. **c**, **f**, Vehicle-treated mice, after CHI. Excessive neuronal loss was the most characteristic finding, additionally to ischaemic (arrows) and necrotic neurons (arrowheads).

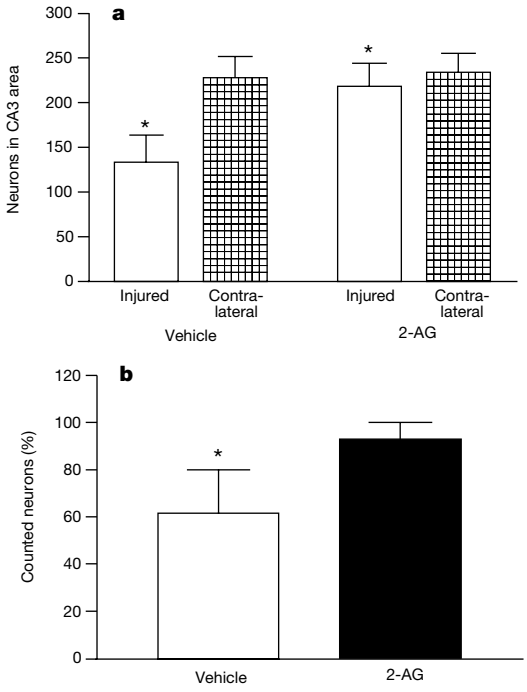

Figure 4 Effects of 2-AG treatment on the neuronal cell loss in the CA3 hippocampal subfield. **a**, The number of neurons in the injured and contralateral control sides (asterisk, $P < 0.001$). **b**, The number of neurons counted in the CA3 area in the injured hemisphere, expressed as a percentage of those counted in the CA3 area in the intact hemisphere, in vehicle-treated and 2-AG-treated mice (asterisk, $P < 0.001$). Data are mean ± s.d.

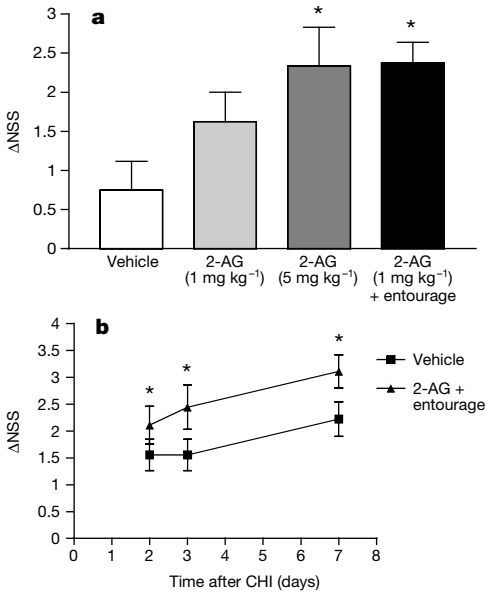

Figure 5 'Entourage' of congeners enhances the effect of 2-AG. **a**, 2-AG was injected 1 h after CHI together with its congeners, 2-palmitoyl-glycerol and 2-linoleoyl-glycerol at a dose ratio of 1, 5 and 10 mg kg^{-1}, respectively. ΔNSS was evaluated at 24 h to assess the protective effect of the mixture compared with the effect of 2-AG at the same dose. Whereas the effect of 1 mg kg^{-1} of 2-AG by itself was not significant, in the presence of the entourage it was more effective, reaching a significant protective effect, comparable to 2-AG at a higher dose (5 mg kg^{-1}). Asterisk, $P < 0.05$ versus control CHI-traumatized mice injected with vehicle. **b**, The 2-AG plus entourage mixture was injected 1, 24 and 48 h after CHI, and its protective effects were sustained for 7 days. Data are mean ± s.e.m.

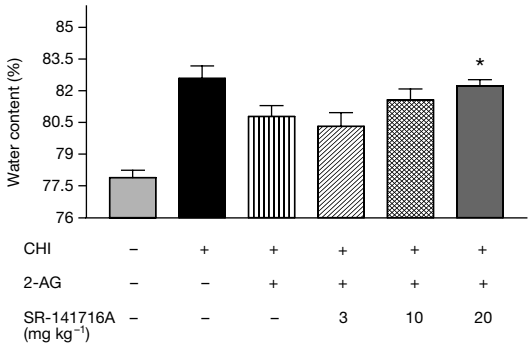

Figure 6 The protective effect of 2-AG is mediated by the CB_1 cannabinoid receptor. SR-141716A is a specific antagonist of the CB_1 brain receptor. Mice were subjected to CHI and 1 h later were injected with 2-AG (1 mg kg^{-1}) and the antagonist (at 3, 10 or 20 mg kg^{-1}). After 24 h they were killed and oedema was assessed. At its highest dose (20 mg kg^{-1}), the antagonist significantly abolished the protective effect of 2-AG, suggesting that the latter affords its protection through its action at the CB_1 receptor. Asterisk, $P < 0.05$ versus 2-AG alone. Data are mean ± s.e.m.

ouabain-induced *in vivo* excitotoxicity[25]. The cytoprotective functions of *N*-acyl ethanol amines, including the endocannabinoid anandamide, have recently been reviewed[26]. Moreover, a non-psychotropic cannabinoid analogue (HU-211), which does not bind to either CB_1 or CB_2 but which has NMDA (*N*-methyl-D-aspartate) blockade properties, has been shown to provide significant protection both *in vivo* and *in vitro*[27], and enhanced production of 2-AG in rat brain administered with picrotoxinin has been recorded[28]. CB_1 agonists are also known to exert anti-inflammatory effects[29] and to cause hypothermia[30]. And, as noted above[9], 2-AG prevents formation of TNF-α and ROS. These mechanisms may contribute towards the neuroprotective profile of 2-AG.

Because cannabinoids are known to reduce body temperature[5], and because hypothermia has been reported to provide neuroprotection, we monitored the effect of 2-AG on body temperature. No reduction of body temperature was found at 0.1 mg kg^{-1} (a dose that abolished oedema) and only minor reduction (~1.6–1.9 °C), too small to exert the observed protection, was noted after administration of 5 mg kg^{-1}. A possible mechanism by which 2-AG may protect the injured brain is related to its ability to abolish the deleterious effect of endothelin-1 (ET-1). ET-1 is the most potent vasoconstrictor known; it reduces cerebral blood flow and is important in the pathophysiology of brain trauma and ischaemia. We recently demonstrated that 2-AG counteracts ET-1-induced cerebral capillary and microvascular endothelial responses (that is, Ca^{2+} mobilization and cytoskeletal rearrangement)[31]. We suggest, therefore, that 2-AG contributes to cerebroprotection not only by reducing neuronal excitotoxicity and inhibiting production of TNF-α and ROS, but also by lowering cerebral vasoconstriction.

In response to traumatic brain injury there is local and transient accumulation of 2-AG at the site of injury, peaking at 4 h and sustained up to at least 24 h. Although the exact role of endogenous 2-AG is yet not known, the neuroprotection exerted by exogenous 2-AG suggests that it may serve as a molecular regulator of pathophysiological events, attenuating excitotoxicity and protecting the brain during development of secondary injury. Inhibition of this protective effect by SR-141716A suggests that 2-AG and the CB_1 receptor may be important in the pathophysiology of traumatic brain injury. However, because of the high dose of the CB_1 antagonist required to block the 2-AG protective effect, a non-CB_1-mediated mechanism of 2-AG cannot be excluded. □

Methods

Animals

The study was performed according to the guidelines of the Institutional Animal Care Committee. Male Sabra mice (Hebrew University strain) weighing 32–35 g were used. The animals were divided into groups, treated with different doses of 2-AG and killed at different times after CHI or sham surgery.

Trauma model

Trauma was induced under ether anaesthesia, which was confirmed by testing loss of pupillary and corneal reflexes, as described previously in detail[12]. To assess the functional impairment after trauma, the NSS scoring system was used based on the ability of the mice to perform ten different tasks that evaluate motor ability, balancing and alertness[13]. Cerebral oedema was evaluated by determining the tissue water content in the injured brain, as previously described[12]. The percentage of water in the tissue was calculated as ((wet weight − dry weight)/wet weight) × 100.

Analysis of brain 2-AG levels

Brains were frozen at the designated post-CHI times. Tissue segments were homogenized in a mixture of chloroform and methanol (2 : 1) containing 10 μl of 1 mM arachidinin as an internal standard. Vacuum filtration was carried out and the filter washed at least three times with the organic mixture. The solvents were evaporated to dryness. The solid residue was re-dissolved in chloroform and dried under nitrogen, and fatty acids were separated from other lipids using thin-layer chromatography (TLC) plates with fluorescent indicator. Synthetic 2-AG in chloroform was applied alongside the analysed fraction to help in the identification of endogenous 2-AG. The solvent system for developing of sample was hexane, ether, acetone and acetic acid (40 : 20 : 7 : 1, v/v). Using a visualizing reagent ($KMnO_4$), the 2-AG was identified, scraped, removed from the silica gel and placed into tubes containing chloroform and methanol (19 : 1); the fractions were collected and evaporated to dryness. The solid residue was dissolved in chloroform and dried under a stream of nitrogen.

GC–MS analysis

We quantitatively analysed the samples by gas chromatography–mass spectrometry (GC–MS) in a Hewlett-Packard G1800A GCD system fitted with a 5% phenylmethylsiloxane (HP-5MS) capillary column (30 m × 0.25 mm (internal diameter) × 0.25 μm), temperature programmed from 150 to 280 °C at 50 °C min^{-1}. The selected qualifier ions were (*m*/*z*) 74, 103 and 129 for 2-AG and 57, 73 and 147 for arachidinin. Quantifier ions were 218 for 2-AG and 427 for arachidinin, respectively. 2-AG amounts of 0.5–16 nmol were used for the calibration curve together with 10 nmol arachidinin.

To the solid residue, which was separated by TLC, dissolved in chloroform and dried again, 10 μl of bis(trimethyl-silyl)trifluoroacetamide (BSTFA) was added to silylate the free hydroxyl groups. Two microlitres of this solution were injected into the GC-MS. 2-AG and the standard arachidinin were eluted after 540 and 620 s, respectively. The ratio between 2-AG and the standard was used to calculate the level of 2-AG in the brain.

Evaluation of infarct volume

Mice were traumatized and treated with vehicle or 2-AG, and after 24 h their brains were sliced every 2 mm using a brain mould. The slices were placed in a 2% solution of 2,3,5-triphenyltetrazolium chloride (TTC) in PBS buffer[14] and photographed with a Stereoscope Stemi SV11 (Zeiss) and digital photocamera Coolpix E990 (Nikon). Scion Image-Release Beta 4.0.2 program was used to quantify the infarct volume.

Evaluation of hippopcampal cell death

Mice were killed by perfusion fixation with 4% phosphate-buffered formaldehyde under ether anaesthesia and brains were post-fixed with the same fixative. Serial 6-μm brain cryostat sections, cut coronally, anterior to posterior, were stained with haematoxylin and eosin and Nissl, and two uninformed observers reviewed the preparations independently. Cell counting was performed under light microscope and camera lucida on the CA3 subfield of dorsal hippocampus in both hemispheres, in 12–15 randomly chosen sections from each brain. By definition, the CA3 area started at the CA3–CA2 border up to the point where the CA3 neurons enter the dentate gyrus, as defined by the lateral aspect of the granule cell layer's dorsal and ventral leaves (Fig. 3a). Ischaemic and necrotic neurons were recognized according to morphological criteria. In an attempt to estimate the neuronal loss in the CA3 area of the injured side, the percentage of the number of neuronal cells counted in this area was evaluated against the contralateral control CA3 subfield. All neurons were included, no matter whether they were normal, ischaemic or necrotic. A paired *t*-test and *t*-tests for independent samples of groups were performed.

Received 17 May; accepted 13 August 2001.

1. Povlishock, J. T. & Christman, C. W. The pathobiology of traumatically induced axonal injury in animals and humans: A review of current thoughts. *J. Neurotrauma* **12,** 555–564 (1995).
2. Kochanek, P. M. *et al.* Biochemical, cellular, and molecular mechanisms in the evolution of secondary damage after severe traumatic brain injury in infants and children: Lessons learned from the bedside. *Pediatr. Crit. Care Med.* **1,** 4–19 (2000).
3. Mechoulam, R. *et al.* Identification of an endogenous 2-monoglyceride, present in canine gut, that binds to cannabinoid receptors. *Biochem. Pharmacol.* **50,** 83–90 (1995).
4. Sugiura, T. *et al.* 2-Arachidonoylglycerol: A possible endogenous cannabinoid receptor ligand in brain. *Biochem. Biophys. Res. Commun.* **215,** 89–97 (1995).
5. Mechoulam, R., Fride, E. & Di Marzo, V. Endocannabinoids. *Eur. J. Pharmacol.* **359,** 1–18 (1998).
6. Piomelli, D., Giuffrida, A., Calignano, A. & Rodriguez de Fonseca, F. The endocannabinoid system as a target for therapeutic drugs. *Trends Pharmacol. Sci.* **21,** 218–223 (2000).
7. Axelrod, J. & Felder, C. C. Cannabinoid receptors and their endogenous agonist, anandamide. *Neurochem. Res.* **23,** 575–581 (1998).
8. McIntosh, T. K., Juhler, M. & Wieloch, T. Novel pharmacologic strategies in the treatment of experimental traumatic brain injury *J. Neurotrauma* **15,** 731–769 (1998).
9. Gallily, R., Breuer, A. & Mechoulam, R. 2-Arachidonylglycerol, an endogenous cannabinoid, inhibits tumor necrosis factor α production in murine macrophages, and in mice. *Eur. J. Pharmacol.* **406,** R5–R7 (2000).
10. Chan, P. H. Reactive oxygen radicals in signaling and damage in the ischemic brain. *J. Cereb. Blood Flow Metab.* **21,** 2–14 (2001).
11. Shohami, E., Ginis, I. & Hallenbeck, J. M. Dual role of tumor necrosis factor α in brain injury. *Cytokines Growth Factor Rev.* **10,** 119–130 (1999).
12. Chen, Y., Constantini, S., Trembovler, V., Weinstock, M. & Shohami, E. An experimental model of closed head injury in mice: Pathophysiology, histopathology and cognitive deficits. *J. Neurotrauma* **13,** 557–568 (1996).
13. Beni-Adani, L. *et al.* A peptide derived from activity-dependent neuroprotective protein (ADNP) ameliorates injury response in closed head injury in mice. *J. Pharmacol. Exp. Ther.* **296,** 57–63 (2001).
14. Mathews, K. S. *et al.* Rapid quantification of ischaemic injury and cerebroprotection in brain slices using densitometric assessment of 2,3,5-triphenyltetrazolium chloride staining. *J. Neurosci. Meth.* **102,** 43–51 (2000).
15. Ben-Shabat, S. *et al.* An entourage effect: Inactive endogenous fatty acid glycerol esters enhance 2-arachidonoyl glycerol cannabinoid activity. *Eur. J. Pharmacol.* **353,** 23–31 (1998).
16. Adams, I. E., Compton, D. R. & Martin, B. R. Assessment of anandamide interaction with the cannabinoid brain receptor: SR141716A antagonism studies in mice and autoradiographic analysis of receptor binding in rat brain. *J. Pharmacol. Exp. Ther.* **284,** 1209–1217 (1998).
17. Smith, S. R., Terminelli, C. & Denhardt, G. Effects of cannabinoid receptor agonist and antagonist ligands on production of inflammatory cytokines and anti-inflammatory interleukin-10 in endotoxemic mice. *J. Pharmacol. Exp. Ther.* **293,** 136–150 (2000).
18. Shohami, E., Shapira, Y., Yadid, G., Reisfeld, N. & Yedgar, S. Brain phospholipase A2 is activated after experimental closed head injury in rats. *J. Neurochem.* **53,** 1541–1546 (1989).
19. Nadler, V., Biegon, A., Beit-Yannai, E., Adamchik, J. & Shohami, E. ^{45}Ca accumulation in rat brain after closed head injury; attenuation by the novel neuroprotective agent HU-211. *Brain Res.* **685,** 1–11 (1995).
20. Reggio, P. H. & Traore, H. Conformational requirements for endocannabinoid interaction with the cannabinoid receptors, the anandamide transporter and fatty acid amidohydrolase. *Chem. Phys. Lipids* **108,** 15–35 (2000).
21. Goparaju, S. K., Ueda, N., Yamaguchi, H. & Yamamoto, S. Anandamide amidohydrolase reacting with 2-arachidonoylglycerol, another cannabinoid receptor ligand. *FEBS Lett.* **422,** 69–73 (1998).
22. Sinor, A. D., Irvin, S. M. & Greenberg, D. A. Endocannabinoids protect cerebral cortical neurons from *in vitro* ischemia in rats. *Neurosci. Lett.* **278,** 157–160 (2000).
23. Shen, M. & Thayer, S. A. Cannabinoid receptor agonists protect cultured rat hippocampal neurons from excitotoxicity. *Mol. Pharmacol.* **54,** 459–462 (1998).
24. Nagayama, T. *et al.* Cannabinoids and neuroprotection in global and focal cerebral ischemia and in neuronal cultures. *J. Neurosci.* **19,** 2987–2995 (1999).
25. van der Stelt, M. *et al.* Neuroprotectin by Delta9-tetrahydrocannabinol, the main active compound in marijuana, against ouabain-induced *in vivo* excitotoxicity. *J. Neurosci.* **21,** 6475–6479 (2001).
26. Hansen, H. S., Moesgaard, B., Hansen, H. H. & Petersen, G. *N*-acylethanolamines and percursor phospholipids—relation to cell injury. *Chem. Phys. Lipids* **108,** 135–150 (2000).
27. Shohami, E. & Mechoulam, R. Dexanabinol (HU-211): A nonpsychotropic cannabinoid with neuroprotective properties. *Drug Develop. Res.* **50,** 211–215 (2000).
28. Sugiura, T., Yoshinaga, N., Kondo, S., Waku, K. & Ishima, Y. Generation of 2-arachidonoylglycerol, an endogenous cannabinoid receptor ligand, in picrotoxinin-administered rat brain. *Biochem. Biophys. Res. Comm.* **271,** 654–658 (2000).
29. Klein, T. W., Lane, B., Newton, C. A. & Friedman, H. The cannabinoid system and cytokine network. *Proc. Soc. Exp. Biol. Med.* **225,** 1–8 (2000).
30. Ovadia, H., Wohlman, A., Mechoulam, R. & Weidenfeld, J. Characterization of the hypothermic effect of the synthetic cannabinoid HU-210 in the rat. Relation to the adrenergic system and endogenous pyrogens. *Neuropharmacology* **34,** 175–180 (1995).
31. Chen, Y. *et al.* Human brain capillary endothelium. 2-Arachidonoylglycerol (endocannabinoid) interacts with endothelin-1. *Circ. Res.* **87,** 323–327 (2000).

Acknowledgements

We thank the US National Institute of Drug Abuse and the Israel Science Foundation for support (grants to R.M.). E.S. and R.M. are affiliated with the David R. Bloom Center for Pharmacy at the Hebrew University of Jerusalem's School of Pharmacy.

Correspondence and requests for materials should be addressed to E.S. (e-mail: esty@cc.huji.ac.il).

A synthetic glycolipid prevents autoimmune encephalomyelitis by inducing T_H2 bias of natural killer T cells

Katsuichi Miyamoto*, Sachiko Miyake* & Takashi Yamamura

Department of Immunology, National Institute of Neuroscience, NCNP, 4-1-1 Ogawahigashi, Kodaira, Tokyo 187-8502, Japan
** These authors contributed equally to this work*

Experimental autoimmune encephalomyelitis (EAE) is a prototype autoimmune disease mediated by type 1 helper T (T_H1) cells and under the control of regulatory cells[1–3]. Here we report that a synthetic glycolipid ligand for CD1d-restricted natural killer T (NKT) cells expressing the semi-invariant T-cell receptor (Vα14$^+$) is preventive against EAE. The ligand is an analogue of α-galactosylceramide (α-GC), a prototype NKT cell ligand, with a truncated sphingosine chain. α-GC causes NKT cells to produce both interferon (IFN)-γ and interleukin (IL)-4 (refs 4, 5). However, this new ligand can induce a predominant production of IL-4 by the NKT cells. A single injection of this glycolipid, but not of α-GC, consistently induced T_H2 bias of autoimmune T cells by causing NKT cells to produce IL-4, leading to suppression of EAE. The lack of polymorphism of CD1d and cross-reactive response of mouse and human NKT cells to the same ligand[6] indicates that targeting NKT cells with this ligand may be an attractive means for intervening in human autoimmune diseases such as multiple sclerosis.

Conventional T cells respond to peptide ligands in the context of the major histocompatibility complex (MHC). In contrast, the CD1d-restricted Vα14$^+$ NKT cells, which express NK cell markers and the T-cell receptor (TCR) with the invariant α-chain[7–9], react to the glycolipid ligand bound to the monomorphic CD1d molecule and produce large amounts of IFN-γ and IL-4 within hours of TCR ligation. Although the natural ligand for NKT cells is unknown, a derivative of marine sponge, α-GC[4,5], is now established as a prototype NKT cell ligand inducing proliferation, cytokine production[4,5] and apoptotic death[10] of NKT cells. According to the trimolecular model of CD1–glycolipid antigen interactions, the TCR of NKT cells is predicted to contact the hydrophilic galactose moiety of α-GC, whereas two aliphatic hydrocarbon chains would